DYNAMICAL ANALYSIS AND FINITE-TIME SYNCHRONIZATION OF A NEW MEMRISTOR-BASED CHAOTIC SYSTEM WITH AMPLITUDE MODULATION

Li-Li Jia, Hai-Yong Cao†

School of Computer and Information Engineering
Nanchang Institute of Technology, Nanchang 330044, China

Received 19 July 2024, accepted 4 December 2024, published online 9 December 2024

A simple one-equilibrium memristor-based chaotic system (MCS) is established by combining a non-ideal memristor with a three-dimensional (3D) chaotic system with six polynomial terms. Its dynamical characteristics are studied and verified by some simulation experiments. The proposed MCS produces chaos via period-doubling bifurcation and maintains steady and robust chaotic behaviors unaffected by initial conditions. By changing the parameter values, the oscillation amplitudes of all the variables will be enlarged or shrunk on a large scale, indicating the existence of large-scale chaotic amplitude modulation. The finite-time synchronization (FTS) of the proposed MCS is studied, and the sufficient conditions of FTS based on simple feedback control are established via strict theoretical analysis. Numerical simulations demonstrate the correctness of the obtained results.

DOI:10.5506/APhysPolB.55.11-A2

1. Introduction

In the field of complexity science, chaos has always been an important topic of continuous attention as it pervades every corner of human society and nature, and displays mysterious influence in their normal operations. The rise of chaos research began with the discovery of the celebrated Lorenz system with butterfly attractor in 1963 [1], and thereafter significant achievements related to the chaos model, control, and application were developed over the past half century. Another landmark event that has inspired the chaos research in recent years is the preparation of the physical memristor in 2008 [2], which truly brought the memristor into the scientific world and opened up the new field of memristor-based chaotic systems (MCSs) and circuits. It is universally acknowledged that the peculiar non-linearity of memristor plays positive effects on chaos generation, thus

† Corresponding author: `flower00@yeah.net`

scholars have shown a growing interest in integrating the memristors into the design of chaotic systems. MCSs are capable of exhibiting complex and potentially applicable dynamics, including chaos, multistability, hidden attractors, offset boosting, amplitude modulation, *etc.* Ioth *et al.* [3] proposed some memristor-based chaotic oscillators by simply substituting the diode of the canonical Chua oscillator for one memristor featured by piecewise-linear and monotone-increasing non-linearities. Muthuswamy [4] implemented the memristor via some off-the-shelf elements and the memristor-based Chua oscillator with a two-scroll chaotic attractor on breadboard, and constructed a simplest memristor-based chaotic circuit composed of a passive inductor, a passive capacitor, and an active memristor [5]. Jin *et al.* [6] put forward a local active memristor and coupled it with a passive inductor and a passive capacitor to establish a new chaotic circuit. Gu *et al.* [7] designed a no-equilibrium four-dimensional (4D) MCS with multiwing attractors and coexisting attractors via numerical and experimental verification. Njimah *et al.* [8] used the memristor emulator with a diode bridge and RC filter to connect a pair of Duffing oscillators for establishing a chaotic system with a four-scroll chaotic attractor and coexisting attractors. Dong and Yang [9] presented a memristor-based hyperchaotic system with hidden chaos and unstable periodic orbit and studied its DSP implementation. Lai *et al.* [10] established an effective method for generating 3D hyperchaotic maps by applying discrete memristors, and studied their performance, realization, and image encryption application. Liu *et al.* [11] designed a family of discrete-time memristor-based chaotic maps with multistability inspired by memristor initial-relied offset boosting, and considered their DSP realization and PRNG application. Memristors can also be used as electromagnetic radiations and synapses to generate memristive neurons and neural networks with chaos. Han *et al.* [12] proposed a chaotic neuron on the basis of a bi-functional memristor and studied its secure communicating application. Lai *et al.* [13] introduced a new memristor as a synapse to construct a memristor-based cyclic neural network with multiscroll chaos and broken infinite coexisting attractors, and showed its superior application in designing chaotic cipher. Liu *et al.* [14] investigated the firing properties of the Rulkov neuron with a charge-controlled memristor for imitating the electromagnetic radiation through energy approaches. Hitherto more MCSs with different model structures and dynamical properties have emerged.

Synchronization refers to the process in which the states of two or more dynamical systems reach a certain consistent behavior via internal or external forces. It was proven to have potential applications in secure communication and thereby many scholars have shown great interest in studying chaos synchronization. Up to now, different synchronization types (such as complete synchronization, lag synchronization, FTS, *etc.*), synchronization control technologies (such as sliding mode control, adaptive control, event-driven control, *etc.*), and related synchronization results have been proposed [15–17]. The difference between FTS and the conventional synchronization concept is that it focuses more on achieving the consensus state within a finite time, determining its better practicality and operability in secure communication. Mishra *et al.* [18] considered the FTS of a multiscroll chaotic system with parameter uncertainties by using a single controller. Sweetha *et al.* [19] investigated the FTS of a delayed fractional-order chaotic system with disturbances, quantization, uncertainties, actuator faults, and derived the FTS results in theoretical ways. Recently, the FTS of MCS has become an upgrading research focus that is still in its early stage and deserves further research.

Chaos generation is the foundation of chaos analysis, implementation, control, and application. In the current situation where artificial and natural chaotic systems have not been fully and completely understood, the generation and analysis of chaotic systems are one of the mainstream directions in chaos research. Simultaneously, there is currently no good unified method for chaos generation, thus it is necessary to make targeted attempts at generating chaotic systems. Moreover, diverse chaotic systems with different structures can bring more possibilities for engineering applications. The emergence of memristors has brought new opportunities and challenges to the generation and analysis of chaotic systems. It is widely believed that memristors have the ability to enhance complexity of chaotic systems and inspire them to show some unknown and interesting features, that is why the researchers generally tend to introduce memristors into chaotic systems. The generation and analysis of MCSs can further deepen the understanding of chaotic systems and promote the application study of memristors in chaotic systems. On the basis of proposing a new MCS with simple structure, this paper provides a comprehensive observation of the dynamical behaviors and FTS of the presented system. The steady chaos and diverse amplitude modulation distinct from some existing chaotic systems are discovered. The FTS of the system is studied and the corresponding synchronization results are established. To the best of our knowledge, the FTS has better practical value than general synchronization, and currently, there are only a few studies discussing the FTS of MCS. The paper is organized as follows. Section 2 gives the model of MCS and evaluates its equilibrium stability. Section 3 analyzes the dynamical behaviors of MCS. Section 4 theoretically studies the FTS of MCS. Section 5 presents the conclusions of the work.

2. System description

Recall an autonomous chaotic system whose mathematical model is composed of four linear and two non-linear terms that can be described as [20]

$$\begin{cases} \dot{x} = z^2 - yz - ay\,, \\ \dot{y} = z\,, \\ \dot{z} = x - z\,. \end{cases} \tag{1}$$

It can yield chaos in phase space $(x, y, z) \in R^3$ by selecting suitable values of parameter a. In order to improve the dynamical properties of system (1), we will introduce the following non-ideal memristor model written as:

$$\begin{cases} i = M(w)u\,, \\ \dot{w} = u - w\,, \\ M(w) = 1 + 0.1w^2\,, \end{cases}$$

where w and $M(w)$ are the internal state and memductance of the memristor, i and u are the terminal current and voltage. The pinched hysteresis loop of the memristor is illustrated in Fig. 1. Based on literature [21, 22], an important feature of the memristor is that its i–u characteristic curve is an 8-shaped pinched hysteresis loop that contracts toward the origin, which can partially reflect the memory function of the memristor.

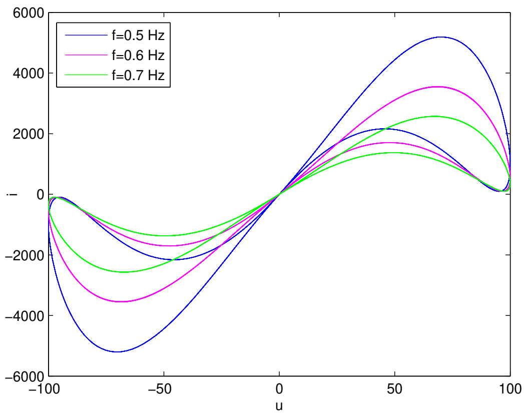

Fig. 1. Pinched hysteresis loop of the memristor with frequency $f = 0.5, 0.6, 0.7$ Hz.

Thus, the newly constructed system with a memristor can be written as

$$\begin{cases} \dot{x} = z^2 - yz - ay\,, \\ \dot{y} = kM(w)z\,, \\ \dot{z} = bx - z\,, \\ \dot{w} = z - w\,, \end{cases} \tag{2}$$

where a, b, k are all positive parameters. Both the system (2) and system (1) are dissipative with only one equilibrium. However, the introduction of memristor and the increase in dimensionality make it possible for system (2) to generate more diverse dynamical behaviors.

In terms of chaotic characteristics, system (2) is more prone to generating continuous and steady chaotic behavior than system (1), and its chaotic parameter region is larger. Owing to the special non-linear features of the memristor, system (2) has the possibility to generate chaotic sequences with better randomness for enhancing the encryption application. Simulations show that system (2) exhibits multi-parameter, multi-variable, and large-scale amplitude modulation, which is difficult to be detected in system (1). Thus, system (2) exhibits stronger parameter-based signal control capability than system (1). In the next part, we will numerically study the dynamical behaviors of system (2) and theoretically establish its finite-time synchronization conditions.

By linearizing system (2) at the equilibrium $O(0,0,0,0)$, the characteristic equation is obtained

$$(\lambda+1)\left(\lambda^3+\lambda^2+abk\right)=0\,. \tag{3}$$

Accordingly, O is an unstable equilibrium. For $a=0.8$, $b=1$, and $k=1$, the eigenvalues of Eq. (3) are calculated as $\lambda_1=-1$, $\lambda_2=-1.4052$, and $\lambda_{3,4}=0.2026\pm0.7268i$ implying the instability of equilibrium, and single-scroll attractor around the equilibrium is observed from initial value (0.1,0.1,0.1,0.1), as illustrated in Fig. 2.

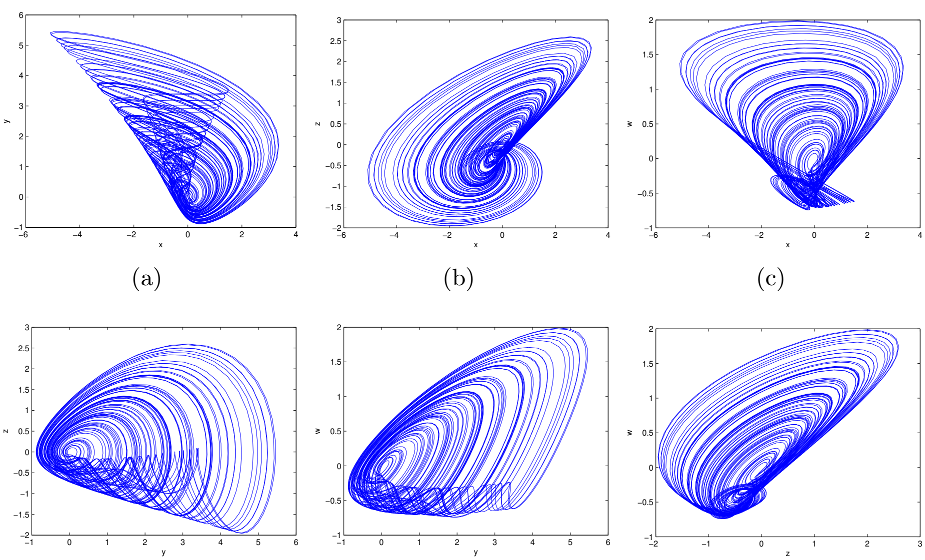

(a) (b) (c)

(d) (e) (f)

Fig. 2. Chaotic attractor in different phase planes with parameters $a=0.8$, $b=1$, $k=1$: (a) $x-y$; (b) $x-z$; (c) $x-w$; (d) $y-z$; (e) $y-w$; (f) $z-w$.

3. Dynamical analysis

This section will show the route to chaos and amplitude modulation of chaotic signals of system (2) via simulation experiments with the fourth-fifth-order Runge–Kutta integrator with a fixed step size of $\Delta t = 0.01$ and the initial value $(x(0), y(0), z(0), w(0)) = (0.1, 0.1, 0.1, 0.1)$. By selecting the parameters $a = 1$, $k = 1$, and varying parameter b within $[0.1, 1.4]$, the bifurcation diagram and Lyapunov exponents (LEs) of system (2) are numerically drawn in Fig. 3, which, to some extent, displays its parameter-relied dynamical evolution process. It is clear that system (2) follows the pattern of period-doubling bifurcation to yield chaos, and undergoes period, chaos, period and ultimately almost maintains chaos with the increase of b. Fixed $b = 0.1, 0.2, 0.3, 0.5, 0.63, 0.69, 0.9, 1, 1.4$, the phase portraits with respect to periodic-1, periodic-2, periodic-4, and chaotic attractors are given in Fig. 4 which visually verify the chaos generation and attractor switching of system (2) accompanied by parameter changes.

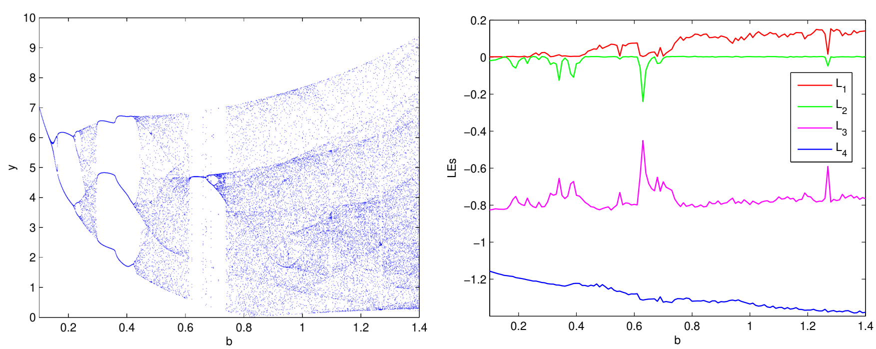

(a) (b)

Fig. 3. Dynamical evolution for $b \in [0.1, 1.4]$: (a) bifurcation diagram; (b) LEs.

Given $a = 1$, $k = 1$, and $b = 1$, we can generate the bifurcation diagrams, respectively, from the initial states $y(0) \in [0, 100]$, $w(0) \in [0, 100]$ as illustrated in Fig. 5. The bifurcation diagrams remain almost unchanged with the variation of $w(0)$, which indicates that the initial condition has no essential impact on the final state of system (2). This, to some extent, reveals that system (2) can generate steady chaotic motion that is independent of initial conditions, exhibiting strong robustness of chaos.

The bifurcation diagram and LEs *versus* the parameter $k \in [1, 3.8]$ can also be plotted by fixing parameters $a = 0.8$ and $b = 1$. As shown in Fig. 6 (a), the local maximum values of y are constantly increasing when k increases. It implies that the boundaries of the attractors and the oscillation amplitudes of variables are expanded, leading to the emergence of chaotic

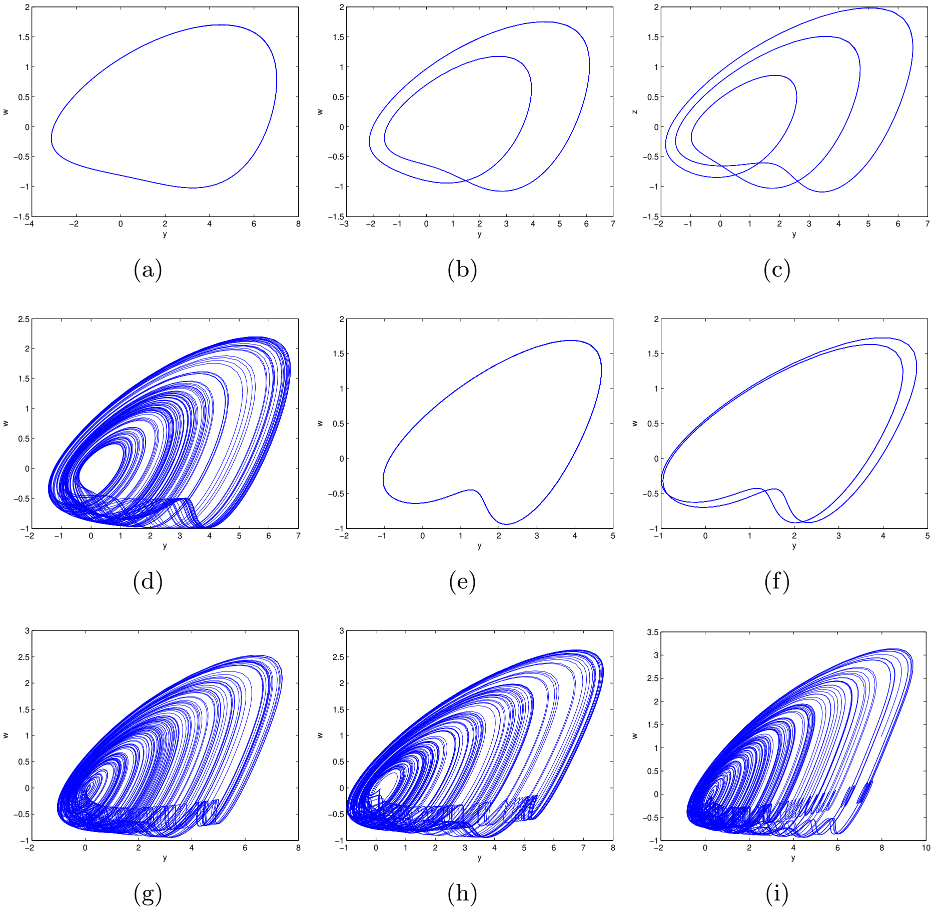

Fig. 4. Phase portraits of system (2): (a) periodic-1 with $b = 0.1$; (b) periodic-2 with $b = 0.2$; (c) periodic-4 with $b = 0.3$; (d) chaotic with $b = 0.5$; (e) periodic-1 with $b = 0.63$; (f) periodic-2 with $b = 0.69$; (g) chaotic with $b = 0.9$; (h) chaotic with $b = 1$; (i) chaotic with $b = 1.4$.

amplitude modulation in system (2). The chaotic amplitude modulation can be visually demonstrated by using the phase portraits and time series with given parameter values of $k = 1.0, 2.5, 3.0, 3.5$. Figure 7 shows that the chaotic feature and attractor shape do not change but the size of the attractor and the amplitude of the time series of y change for different values of k. In fact, it is not difficult to verify that all other variables x, y, w uniformly occur amplitude modulation phenomenon.

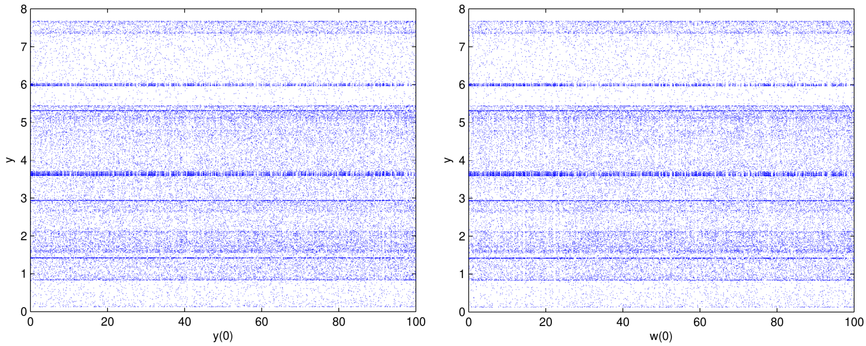

(a) (b)

Fig. 5. Dynamical evolution for $w(0) \in [0, 100]$: (a) bifurcation diagram; (b) LEs.

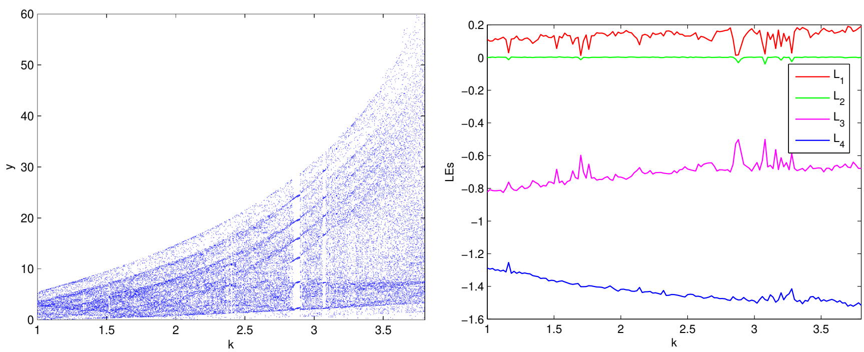

(a) (b)

Fig. 6. Dynamical evolution for $k \in [1, 3.8]$: (a) bifurcation diagram; (b) LEs.

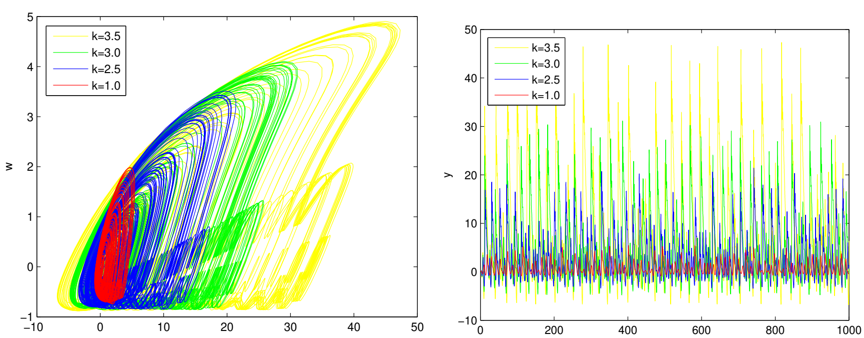

(a) (b)

Fig. 7. Amplitude modulation of attractors for $k = 1.0, 2.5, 3.0, 3.5$: (a) projection on y–w; (b) time series of y.

For $k = 1$, $b = 1$, and $a \in [1, 8]$, the amplitude modulation with respect to parameter a can also be observed from the bifurcation diagram in Fig. 8, which shows that the local maximum values of variable y will be expanded

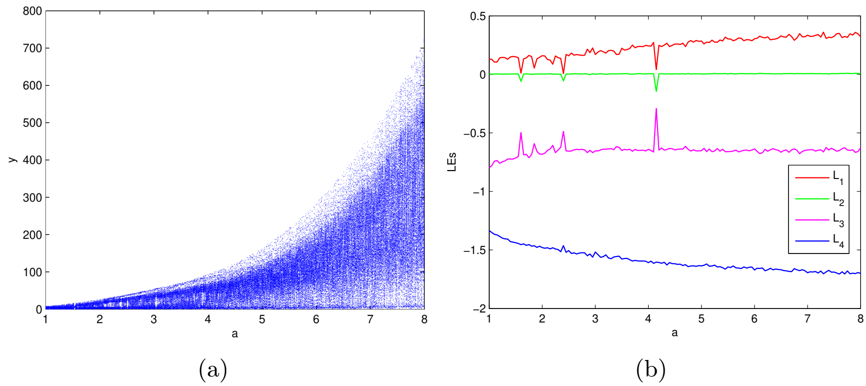

Fig. 8. Dynamical evolution for $a \in [1, 8]$: (a) bifurcation diagram; (b) LEs.

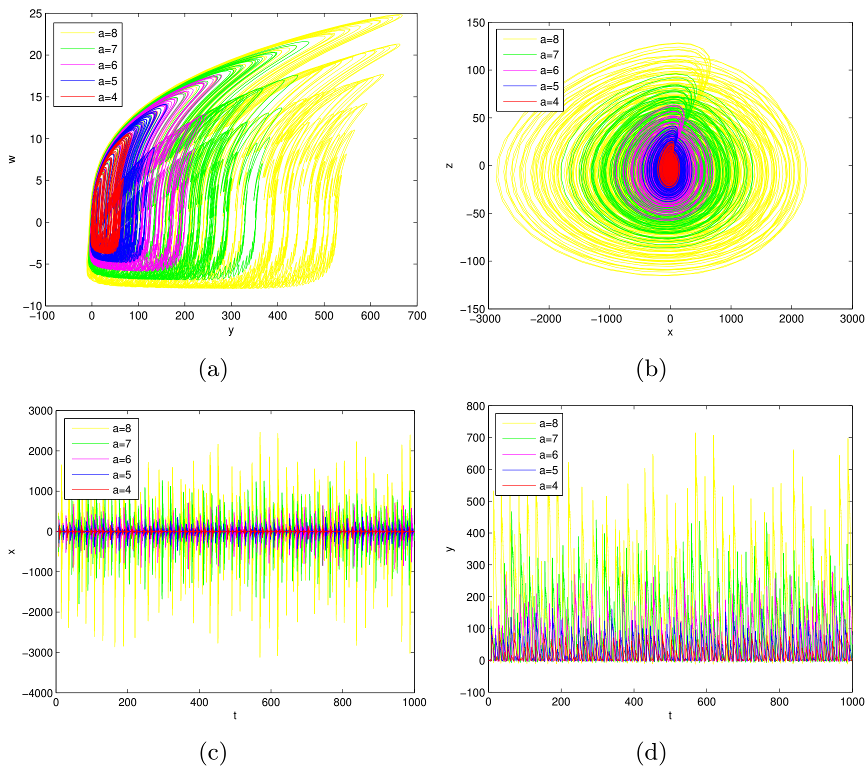

Fig. 9. Dynamical evolution for $a \in [1, 8]$: (a) bifurcation diagram; (b) LEs.

from 0 to nearly 700 with the increase of a. Other variables x, z, and w of system (2) undergo similar changes as well. By selecting $a = 4, 5, 6, 7, 8$, we can plot the projection diagrams of attractors and time series of variables as shown in Fig. 9. The constantly expanding motion regions of attractors and amplified oscillation amplitudes of variables in Fig. 8 with respect to the parameter a indicate the existence of chaotic amplitude modulation of system (2). Actually, system (2) will perform larger scale amplitude modulation as parameters continue to increase.

4. Finite-time synchronization

The FTS which generally refers to all the states of two or more dynamical systems reaches synchronization within a finite time depending on initial conditions, and parameters have better practical value in engineering fields than normal synchronization types. Thus, this section will investigate the FTS of system (2) via the analytical method with numerical verification.

Taking system (2) as the drive system, and assuming that the response system has the same mathematical expression as system (2) with variables (x_1, y_1, z_1, w_1) and control inputs (u_1, u_2, u_3, u_4), it can be written as follows:

$$\begin{cases} \dot{x}_1 = z_1^2 - y_1 z_1 - a y_1 + u_1\,, \\ \dot{y}_1 = kM(w_1) z_1 + u_2\,, \\ \dot{z}_1 = b x_1 - z_1 + u_3\,, \\ \dot{w}_1 = z_1 - w_1 + u_4\,. \end{cases} \tag{4}$$

Denote the errors of variables as $e_1 = x_1 - x$, $e_2 = y_1 - y$, $e_3 = z_1 - z$, and $e_4 = w_1 - w$, then the corresponding error system can be derived as

$$\begin{cases} \dot{e}_1 = (z + z_1 - y_1) e_3 - (z + a) e_2 + u_1\,, \\ \dot{e}_2 = kM(w_1) e_3 + 0.1 k z (w + w_1) e_4 + u_2\,, \\ \dot{e}_3 = b e_1 - e_3 + u_3\,, \\ \dot{e}_4 = e_3 - e_4 + u_4\,. \end{cases} \tag{5}$$

It is clear that the FTS synchronization problem of system (2) and system (4) is transformed into the finite-time stability problem of the error system (5). Based on the finite-time theory, if there exists a constant $T > 0$ such that $\lim_{t\to T} |e_i| = 0$ and $|e_i| \equiv 0$, $i = 1, 2, 3, 4$ when $t \geq T$, then we can say that system (2) and system (4) reach the FTS. Here, we will first introduce some Lemmas for facilitating the establishment of the FTS results.

Lemma 1. *If there exists differential positive function $V(t)$ such that $\dot{V}(t) + cV^{\eta}(x) \leq 0$ for any $c > 0$, $0 < \eta < 1$ and $V(t) \equiv 0$ with $t \geq T$, then the inequality $T(x_0) \leq V^{1-\eta}(x_0)/(c - c\eta)$ with initial condition x_0 holds.*

Proof. Since $\dot{V}(t) + cV^{\eta}(x) \leq 0$, then one has $\mathrm{d}V(t)/V^{\eta}(t) \leq -cdt$. Integrating it in time region $[t_0, T]$, we get

$$\int_{t_0}^{T} \frac{\mathrm{d}V(t)}{V^{\eta}(t)} \leq -c\int_{t_0}^{T} \mathrm{d}t\,, \qquad V^{1-\eta}(T) \leq V^{1-\eta}(t_0) - c(1-\eta)(T-t_0)\,. \tag{6}$$

Thereby, it can be concluded that $V(t) \equiv 0$ with $t \geq T$ and $T(x_0) \leq V^{1-\eta}(x_0)/(c - c\eta)$. The proof is completed. $\square$

Lemma 2. *For real numbers $\tau_1, \tau_2, \cdots, \tau_n$, the inequality $\sum_{j=1}^{n} |\tau_j|^r \leq (\sum_{j=1}^{n} |\tau_j|\,)^r$ with any constant $r > 1$ holds.*

Lemma 3. *For real numbers $\tau_1, \tau_2, \cdots, \tau_n$, the inequality $(\sum_{j=1}^{n} |\tau_j|^2)^{\frac{\mu+1}{2}} \leq \sum_{j=1}^{n} |\tau_j|^{\mu+1}$ with any constant $0 < \mu < 1$ holds.*

Theorem 1. *System (2) and system (4) will achieve FTS with the following controller:*

$$\begin{cases} u_1 = -m\,\mathrm{sgn}(e_1)|e|^{\beta} - (z + z_1 - y_1)e_3 + (z + a)e_2\,, \\ u_2 = -m\,\mathrm{sgn}(e_2)|e|^{\beta} - kM(w_1)e_3 - 0.1kz(w + w_1)e_4\,, \\ u_3 = -m\,\mathrm{sgn}(e_3)|e|^{\beta} - be_1\,, \\ u_4 = -m\,\mathrm{sgn}(e_4)|e|^{\beta} - e_3 \end{cases} \tag{7}$$

and the finite time T satisfies the inequality

$$T \leq \frac{V^{\frac{1-\beta}{2}}(0)}{2^{\frac{\beta-1}{2}} m(1-\beta)}\,, \qquad 0 < \beta < 1\,, \qquad m \text{ is any constant}\,. \tag{8}$$

Proof. Selecting the Lyapunov function as

$$V(t) = \frac{1}{2}\sum_{i=1}^{4} e_i^2 \tag{9}$$

and differentiating $V(t)$, we can get

$$\begin{aligned} \dot{V}(t) \;&=\; \sum_{i=1}^{4} e_i \dot{e}_i = e_1\left[(z + z_1 - y_1)e_3 - (z + a)e_2 + u_1\right] \\ &+e_2\left[kM(w_1)e_3 + 0.1kz(w + w_1)e_4 + u_2\right] \\ &+e_3\left(be_1 - e_3 + u_3\right) + e_4\left(e_3 - e_4 + u_4\right)\,. \end{aligned} \tag{10}$$

Substituting the controller (7) into the above equation, we have

$$\begin{aligned}
\dot{V}(t) &= e_1e_3(z+z_1-y_1)-(z+a)e_1e_2+e_1\Big(-m\,\mathrm{sgn}(e_1)|e_1|^{\beta} \\
&\quad -(z+z_1-y_1)e_3+(z+a)e_2\Big)+e_2\left(-m\,\mathrm{sgn}(e_2)|e_2|^{\beta}\right) \\
&\quad -e_3^2-e_3\left(-m\,\mathrm{sgn}(e_3)|e_3|^{\beta}-be_1\right)-e_4^2 \\
&\quad -e_4\left(-m\,\mathrm{sgn}(e_4)|e_4|^{\beta}-e_3\right) \\
&= -e_3^2-e_4^2-m\left(|e_1|^{\beta+1}+|e_2|^{\beta+1}+|e_3|^{\beta+1}+|e_4|^{\beta+1}\right) \\
&\leq -m\left(|e_1|^{\beta+1}+|e_2|^{\beta+1}+|e_3|^{\beta+1}+|e_4|^{\beta+1}\right). \qquad (11)
\end{aligned}$$

Based on Lemma 2 and Lemma 3, we can get that

$$\dot{V}(t) \leq -m\left(|e_1|^2+|e_2|^2+|e_3|^2+|e_4|^2\right)^{\frac{\beta+1}{2}} \qquad (12)$$

$$\leq -m(2V(t))^{\frac{\beta+1}{2}}. \qquad (13)$$

Therefore, system (2) and system (4) can realize synchronization in a finite time according to Lemma 1, and the finite time is given by inequality (8). The proof is completed. □

We can verify the effectiveness of Theorem 1 via some simulations. When $a = 0.8$, $b = 1$, and $k = 1$, system (2) is chaotic from the initial value $(0.1, 0.1, 0.1, 0.1)$ with its phase portraits shown in Fig. 2. Let the initial value of system (4) be $(-1, 2, 2, -1)$ and control parameters $m = 5$, $\beta = 0.6$, then we can compute that the finite time $T \leq 0.946$ according to Theorem 1. The errors $e_1(t)$, $e_2(t)$, $e_3(t)$, and $e_4(t)$ approach zero as shown in Fig. 10

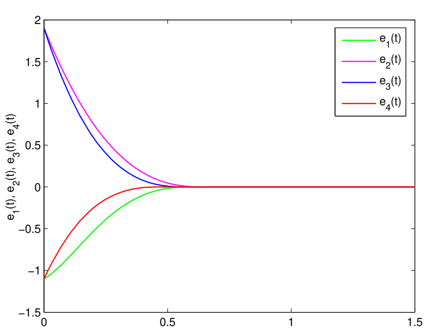

Fig. 10. Errors $e_1(t)$, $e_2(t)$, $e_3(t)$, and $e_4(t)$ of system (2) and system (4).

and all the variables of system (2) and system (4) reach consensus within the finite time T as shown in Fig. 11, which demonstrates the achievement of FTS in accordance with Theorem 1.

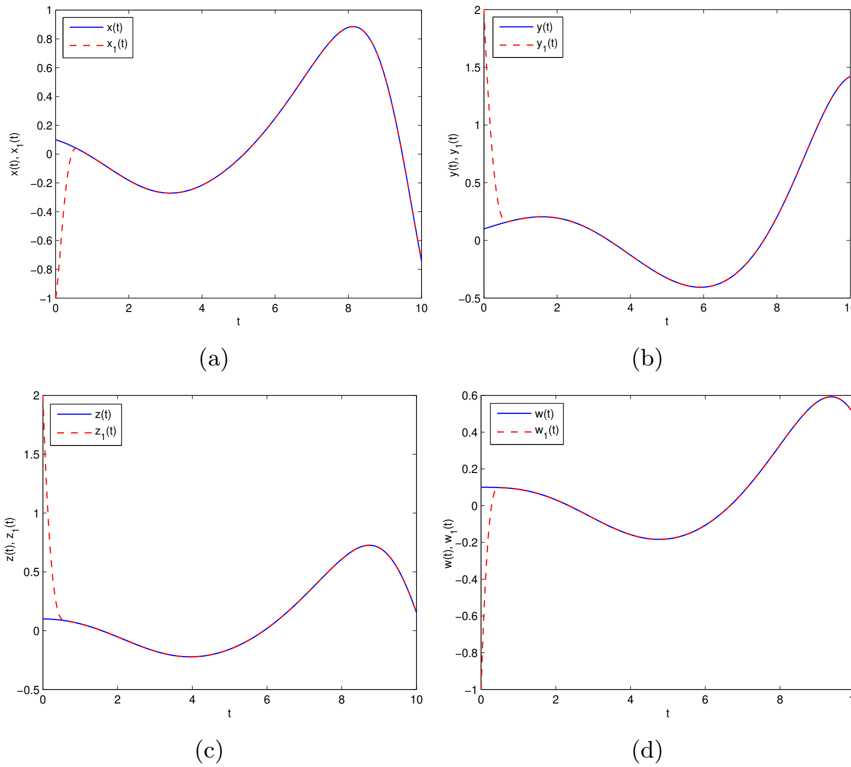

Fig. 11. State variables of system (2) and system (4): (a) $x(t)$, $x_1(t)$; (b) $y(t)$, $y_1(t)$; (c) $z(t)$, $z_1(t)$; (d) $w(t)$, $w_1(t)$.

5. Conclusions

This paper tried to create a simple chaotic model with rich dynamics by combining the memristor to a 3D chaotic flow. The presented MCS in this paper has a simple mathematical model with the non-ideal memristor and only one equilibrium. The dynamical properties including the chaotic attractor, period-doubling bifurcation, and parameter-relied amplitude modulation of the MCS were numerically analyzed. It was shown that all the variables of the MCS can be enlarged or shrunk on a large scale with the change of parameter values. The FTS problem of the MCS was studied and the sufficient conditions for achieving FTS were constructed via theoretical and numerical means. In the future, we will further focus on the model, control and engineering application of MCS. The MCSs with more memristors and complex dynamics (such as hyperchaos, multiscroll attractors, *etc.*) will be yielded, and their stability and synchronization control under different constraints will be studied. Furthermore, more potential application aspects of MCS will be discovered.

REFERENCES

[1] E.N. Lorenz, «Deterministic Nonperiodic Flow», *J. Atmos. Sci.* **20**, 130 (1963).

[2] D.B. Strukov, G.S. Snider, D.R. Stewart, R.S. Williams, «The missing memristor found», *Nature* **453**, 80 (2008).

[3] M. Itoh, L.O. Chua, «Memristor Oscillators», *Int. J. Bifurcation Chaos* **18**, 3183 (2008).

[4] B. Muthuswamy, «Implementing Memristor Based Chaotic Circuits», *Int. J. Bifurcation Chaos* **20**, 1335 (2010).

[5] B. Muthuswamy, L.O. Chua, «Simplest Chaotic Circuit», *Int. J. Bifurcation Chaos* **20**, 1567 (2010).

[6] P. Jin, G. Wang, H.H.C. Iu, T. Fernando, «A Locally Active Memristor and Its Application in a Chaotic Circuit», *IEEE Trans. Circuits Syst. II Express Briefs* **65**, 246 (2018).

[7] S. Gu, Q. Peng, X. Leng, B. Du, «A novel non-equilibrium memristor-based system with multi-wing attractors and multiple transient transitions», *Chaos* **31**, 033105 (2021).

[8] O.M. Njimah *et al.*, «Coexisting oscillations and four-scroll chaotic attractors in a pair of coupled memristor-based Duffing oscillators: Theoretical analysis and circuit simulation», *Chaos, Solitons Fractals* **166**, 112983 (2023).

[9] C. Dong, M. Yang, «A novel 4D memristor-based hyperchaotic system with hidden attractors: Dynamics, periodic orbits analysis, and DSP realization», *Chin. J. Phys.* **89**, 930 (2024).

[10] Q. Lai, L. Yang, G. Chen, «Design and Performance Analysis of Discrete Memristive Hyperchaotic Systems With Stuffed Cube Attractors and Ultraboosting Behaviors», *IEEE Trans. Ind. Electron.* **71**, 7819 (2024).

[11] X. Liu, K. Sun, H. Wang, S. He, «A class of novel discrete memristive chaotic map», *Chaos, Solitons Fractals* **174**, 113791 (2023).

[12] Z. Han, B. Sun, S. Banerjee, J. Mou, «Biological neuron modeling based on bifunctional memristor and its application in secure communication», *Chaos, Solitons Fractals* **184**, 115020 (2024).

[13] Q. Lai, Z. Wan, H. Zhang, G. Chen, «Design and Analysis of Multiscroll Memristive Hopfield Neural Network With Adjustable Memductance and Application to Image Encryption», *IEEE Trans. Neural Networks Learn. Syst.* **34**, 7824 (2023).

[14] B. Liu, X. Peng, C. Li, «Firing behaviors of memristor-based Rulkov neuron map using energy method», *AEU — Int. J. Electr. Commun.* **178**, 155283 (2024).

[15] W. Shammakh, E.E. Mahmoud, B.S. Kashkari, «Complex modified projective phase synchronization of nonlinear chaotic frameworks with complex variables», *Alex. Eng. J.* **59**, 1265 (2020).

[16] M. Asadollahi, A.R. Ghiasi, M.A. Badamchizadeh, «Adaptive synchronization of chaotic systems with hysteresis quantizer input», *ISA Trans.* **98**, 137 (2020).

[17] J. Luo, X. Chen, «Transmission synchronization of multiple memristor chaotic circuits via single input controller and its application in secure communication», *Integration* **90**, 40 (2023).

[18] A.K. Mishra, S. Das, V.K. Yadav, «Finite-time synchronization of multi-scroll chaotic systems with sigmoid non-linearity and uncertain terms», *Chin. J. Phys.* **75**, 235 (2022).

[19] S. Sweetha, R. Sakthivel, S. Harshavarthini, «Finite-time synchronization of nonlinear fractional chaotic systems with stochastic actuator faults», *Chaos, Solitons Fractals* **142**, 110312 (2021).

[20] C.B. Li, J.C. Sprott, «Variable-boostable chaotic flows», *Optik* **127**, 10389 (2016).

[21] L.O. Chua, «If it's pinched it's a memristor», *Semicond. Sci. Technol.* **29**, 104001 (2014).

[22] Y.V. Pershin, M. Di Ventra, «A simple test for ideal memristors», *J. Phys. D: Appl. Phys.* **52**, 01LT01 (2019).